Synthesis, Characterization, Properties, and Asymmetric Catalytic Diels−Alder Reactions of Chiral-at-Metal Imino−Iridium(III) Complexes

Daniel Carmona,* Fernando J. Lahoz, Sergio Elipe, and Luis A. Oro

Departamento de Química Inorgánica, Instituto de Ciencia de Materiales de Aragón, Universidad de Zaragoza-Consejo Superior de Investigaciones Científicas, 50009 Zaragoza, Spain

M. Pilar Lamata, Fernando Viguri, and Carlos Mir

Departamento de Química Inorgánica, Escuela Universitaria de Ingeniería Técnica Industrial, Instituto de Ciencia de Materiales de Aragón, Universidad de Zaragoza-Consejo Superior de Investigaciones Científicas, Corona de Aragón 35, 50009 Zaragoza, Spain

Carlos Cativiela* and M. Pilar López-Ram de Víu

Departamento de Química Orgánica, Instituto de Ciencia de Materiales de Aragón, Universidad de Zaragoza-Consejo Superior de Investigaciones Científicas, 50009 Zaragoza, Spain

Received February 19, 1998

The synthesis and characterization of optically active imino complexes (R_{Ir},R_C)- and (S_{Ir},R_C)-[(η^5-C_5Me_5)IrCl(imine)][SbF_6] (imine = L_n = *N*-(2-pyridylmethylene)−(*R*)-1-phenylethylamine (L_1; **1a,a′**), *N*-(2-pyridylmethylene)-(*R*)-1-naphthylethylamine (L_2; **2a,a′**), *N*-(2-quinolylmethylene)−(*R*)-1-naphthylethylamine (L_3; **3a,a′**), *N*-(6-methyl-2-pyridylmethylene)−(*R*)-1-naphthylethylamine (L_4; **4a,a′**), *N*-(2-pyridylmethylene)−(*R*)-1-cyclohexylethylamine (L_5; **5a,a′**), *N*-(2-pyridylmethylene)−(1*R*,2*S*,4*R*)-1-bornylamine) (L_6; **6a,a′**)), (R_{Ir},R_C)- and (S_{Ir},R_C)-[(η^5-C_5Me_5)IrCl(L_2)][A] (A = Cl (**7a,a′**), BF_4 (**8a,a′**), PF_6 (**9a,a′**), (*1S*)-camphor-10-sulfonate (R*SO_3) (**10a,a′**)) and (R_{Ir},R_C)- and (S_{Ir},R_C)-[(η^5-C_5Me_5)(L_6)(H_2O)][SbF_6]$_2$ (**11a,a′**)) are reported. The absolute crystal structures of (R_{Ir},R_C)-**1a**, (R_{Ir},R_C)-**2a**, and (R_{Ir},R_C)-**3a** were determined by X-ray analysis. All three complexes show the chiral metal center in a pseudo-octahedral environment, being bonded to an η^5-C_5Me_5 ring, to a terminal chloride, and, in a chelate fashion, to the two nitrogen atoms of the imine ligands. For the chloride compounds **1**−**6**, ^{1}H NMR solution data reveal conformational differences between the crystal and solution structures. At room temperature, in acetone, complexes **1**−**11** are configurationally stable. At 62 °C, in methanol, the more labile chloro complex **5a** epimerizes at Ir with a half-life of 68.0 min (activation parameters, $\Delta H^{\ddagger}$ = 97.7 ± 13.2 kJ mol^{-1} and $\Delta S^{\ddagger}$= −26.3 ± 6.2 J K^{-1}mol^{-1}; equilibrium constant, **5a′**/**5a** = 4.26 ± 1.65). Dichloromethane/acetone solutions of the solvate complexes [(η^5-C_5Me_5)Ir(imine)S][SbF_6]$_2$, prepared in situ by treating complexes **1**−**6** with equimolar amounts of $AgSbF_6$, are active catalysts for the Diels−Alder reaction between methacrolein and cyclopentadiene. The reaction occurs rapidly at room temperature with good exo:endo selectivity (84:16 to 95:5) and moderate enantioselectivities (up to 46%).

Introduction

Optically active transition-metal complexes are an important class of compounds because of their potential application in stoichiometric[1] or catalytic[2,3] enantioselective organic synthesis. Among this class of compounds, organometallic complexes containing stereogenic metal centers are ideally suited to obtain mechanistic information about the stereochemical course of reactions, allowing us to improve the understanding of the factors affecting the stereocontrol in enantioselective catalysis.[1,4] Usually these complexes have pseudo-octahedral geometries with η^5-C_5R_5 or η^6-C_6R_6 groups

(1) (a) Brunner, H. *Acc. Chem. Res.* **1979**, *12*, 250. (b) Brunner, H. *Top. Curr. Chem.* **1980**, *56*, 67. (c) Brunner, H. *Adv. Organomet. Chem.* **1980**, *18*, 151.

(2) Brunner, H.; Zettlmeier, W. *Handbook of Enantioselective Catalysis*; VCH: Weinheim, Germany, 1993.

(3) (a) *Catalytic Asymmetric Synthesis*; Ojima, I., Ed.; VCH: Weinheim, Germany, 1993. (b) Noyori, R. *Asymmetric Catalysis in Organic Synthesis*; John Willey and Sons: New York, 1994.

(4) (a) Organometallic Compounds and Optical Activity. *J. Organomet. Chem.* **1989**, *370* (Brunner, H., Vol. Ed.). (b) Meyer, O.; Arif, A. M.; Gladysz, J. A. *Organometallics* **1995**, *14*, 1844 and references therein. (c) Consiglio, G.; Morandini, F. *Chem. Rev.* **1987**, *87*, 761. (d) Johnson, T. J.; Alvey, L. J.; Brady, M.; Mayne, C. L.; Arif, A. M.; Gladysz, J. A. *Chem. Eur. J.* **1995**, *1*, 294 and references therein. (e) Brookhardt, M.; Timmers, D.; Tucker, J. R.; Williams, G. D.; Husk, G. R.; Brunner, H.; Hammer, B. *J. Am. Chem. Soc.* **1983**, *105*, 6721. (f) Sokolov, V. I. *Chirality and Optical Activity in Organometallic Compounds*; Gordon and Breach Science Publishers: New York, 1990. (g) *Asymmetric Synthesis;* Morrison, J. D., Ed; Academic Press: Orlando, FL, 1985; Vol. 5. (h) *Asymmetric Catalysis*; Bosnich, B., Ed; Martinus Nijhoff Publishers: Dordrecht, The Netherlands, 1986. (i) Davies, S. G. *Pure Appl. Chem.* **1988**, *60*, 40. (j) Davies, S. G. *Aldrichimica Acta* **1990**, *23*, 31. (k) Faller, J. W.; Chase, K. J. *Organometallics* **1995**, *14*, 1592.

S0276-7333(98)00112-5 CCC: $15.00
Publication on Web 06/11/1998

occupying three *fac* coordination sites, and some of them contain optically active ligands such as α-amino acids,[5] chiral imines,[6] bis(oxazolines),[7] carbenes,[8] diphosphines,[4c,9] or the chiral chelating C,N ligand *N*,*N*-dimethylphenylethylamine.[10]

Chiral chelating imino complexes have been used as enantioselective catalysts in different organic processes,[2] and in particular, in-situ-generated pseudo-octahedral areneruthenium species with this type of ligands gave moderate enantiomeric excesses in the hydrogen transfer reaction from 2-propanol to alkyl aryl ketones.[11] For these half-sandwich ruthenium compounds it has been shown that N,N chelate imine ligands increase the configurational stability at the metal with respect to N,O-coordinated salicylaldiminato or α-amino acidato anions.[6f]

On the other hand, one of the fundamental reactions for the enantioselective synthesis of organic compounds is the catalytic asymmetric Diels−Alder reaction. It is well-documented that catalysts for this reaction are mainly based on chiral ligands attached to Lewis acids.[3,12] Although, very recently, some transition-metal and lanthanide complexes have been described as promising catalysts for these reactions,[9b,13] as far as we know no chiral imino−transition-metal compounds have been used as catalyst precursors in enantioselective Diels−Alder reactions.

Scheme 1

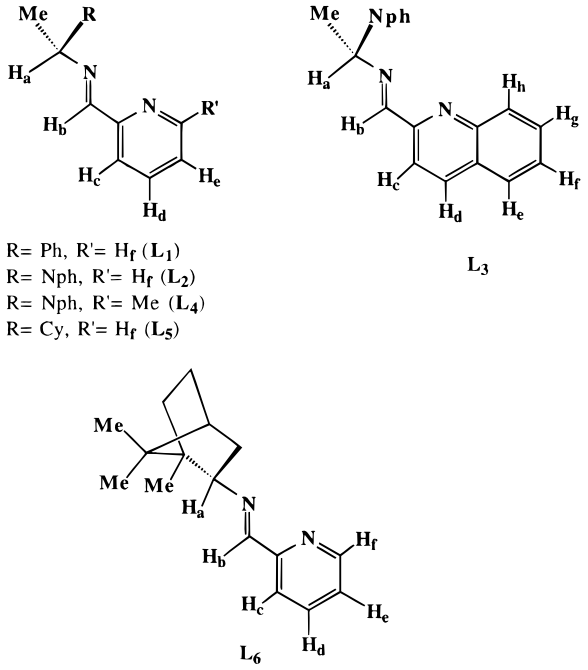

Following our studies on transition-metal complexes with chiral metal centers,[5j,k,9,13i,14] we report in this paper the synthesis and characterization of pseudo-octahedral complexes of general formula $[(\eta^5\text{-}C_5Me_5)\text{-}IrCl(imine)]^+$ containing enantiopure chiral imine ligands (imine = L_1−L_6, Scheme 1). The presence of chiral auxiliaries of known absolute configuration permitted us to assign the absolute configuration at the metal by X-ray diffraction and circular dichroism. The configurational stability of the imine compounds was also studied as well as their use as enantioselective precatalysts for the Diels−Alder reaction between methacrolein and cyclopentadiene.

Results and Discussion

Synthesis and Characterization of the Diastereomeric Chloro Complexes 1−6. At room temperature, the iridium dimer[15] $[\{(\eta^5\text{-}C_5Me_5)IrCl\}_2(\mu\text{-}Cl)_2]$ reacted, in methanol, with stoichiometric amounts of the imines L_1−L_6 and $NaSbF_6$ to give, in 80−92% chemical yield, diastereomeric mixtures of $[(\eta^5\text{-}C_5Me_5)IrCl(L_n)][SbF_6]$ (**1a,a′-6a,a′**) which differ in the configuration at

(5) (a) Dersnah, D. F.; Baird, M. C. *J. Organomet. Chem.* **1977**, *127*, C55. (b) Sheldrick, W. S.; Heeb, S. *J. Organomet. Chem.* **1989**, *377*, 357. (c) Sheldrick, W. S.; Heeb, S. *Inorg. Chim. Acta* **1990**, *168*, 93. (d) Sheldrick, W. S.; Gleichmann, A. *J. Organomet. Chem.* **1994**, *470*, 183. (e) Krämer, R.; Polborn, K.; Wanjek, H.; Zahn, I.; Beck, W. *Chem. Ber.* **1990**, *123*, 767. (f) Zahn, I.; Wagner, B.; Polborn, K.; Beck, W. *J. Organomet. Chem.* **1990**, *394*, 601. (g) Krämer, R.; Polborn, K.; Robl, C.; Beck, W. *Inorg. Chim. Acta* **1992**, *198−200*, 415. (h) Krämer, R.; Maurus, M.; Bergs, R.; Polborn, K.; Sünkel, K.; Wagner, B.; Beck, W. *Chem. Ber.* **1993**, *126*, 1969. (i) Werner, H.; Daniel, T.; Nürnberg, O.; Knaup, W.; Meyer, U. *J. Organomet. Chem.* **1993**, *445*, 229. (j) Carmona, D.; Mendoza, A.; Lahoz, F. J.; Oro, L. A.; Lamata, M. P.; San José, E. *J. Organomet. Chem.* **1990**, *396*, C17. (k) Carmona, D.; Lahoz, F. J.; Atencio, R.; Oro, L. A.; Lamata, M. P.; San José, E. *Tetrahedron: Asymmetry* **1993**, *4*, 1425. (l) Grotjahn, D. B.; Groy, T. L. *J. Am. Chem. Soc.* **1994**, *116*, 6969. (m) Grotjahn, D. B.; Groy, T. L. *Organometallics* **1995**, *14*, 3669. (n) Grotjahn, D. B.; Joubran, C. *Tetrahedron: Asymmetry* **1995**, *6*, 745. (o) Grotjahn, D. B.; Joubran, C.; Hubbard, J. L. *Organometallics* **1996**, *15*, 1230.

(6) (a) Mandal, S. K.; Chakravarty, A. R. *J. Organomet. Chem.* **1991**, *417*, C59. (b) Mandal, S. K.; Chakravarty, A. R. *J. Chem. Soc., Dalton Trans.* **1992**, 1627. (c) Mandal, S. K.; Chakravarty, A. R. *Inorg. Chem.* **1993**, *32*, 3851. (d) Brunner, H.; Oeschey, R.; Nuber, B. *Angew. Chem., Int. Ed. Engl.* **1994**, *33*, 866. (e) Brunner, H.; Oeschey, R.; Nuber, B. *Inorg. Chem.* **1995**, *34*, 3349. (f) Brunner, H.; Oeschey, R.; Nuber, B. *Organometallics* **1996**, *15*, 3616. (g) Brunner, H.; Oeschey, R.; Nuber, B. *J. Organomet. Chem.* **1996**, *518*, 47. (h) Brunner, H.; Oeschey, R.; Nuber, B. *J. Chem. Soc., Dalton Trans.* **1996**, 1499. (i) Loza, M. L.; Parr, J.; Slawin, A. M. Z. *Polyhedron* **1997**, *16*, 2321. (i) Davies, D. L.; Fawcett, J.; Krafczyk, R.; Russell, D. R. *J. Organomet. Chem.* **1997**, *545/546*, 1351.

(7) Asano, H.; Katayama, K.; Kurosawa, H. *Inorg. Chem.* **1996**, *35*, 5760.

(8) Enders, D.; Gielen, H.; Raabe, G.; Runsink, J.; Teles, J. H. *Chem. Ber.* **1997**, *130*, 1253.

(9) (a) Carmona, D.; Lahoz, F. J.; Oro, L. A.; Lamata, M. P.; Viguri, F.; San José, E. *Organometallics* **1996**, *15*, 2961. (b) Carmona, D.; Cativiela, C.; García-Correas, R.; Lahoz, F. J.; Lamata, M. P.; López, J. A.; López-Ram de Víu, M. P.; Oro, L. A.; San José, E.; Viguri, F. *J. Chem. Soc., Chem. Commun.* **1996**, 1247.

(10) (a) Attar, S.; Nelson, J. H.; Fischer, J.; de Cian, A.; Sutter, J.-P.; Pfeffer, M. *Organometallics* **1995**, *14*, 4559. (b) Attar, S.; Catalano, V. J.; Nelson, J. H. *Organometallics* **1996**, *15*, 2932.

(11) Krasik, P.; Alper, H. *Tetrahedron* **1994**, *50*, 4347.

(12) (a) Oh, T.; Reilly, M. *Org. Prep. Proced. Int.* **1994**, *26*, 129. (b) Kagan, H. B.; Riant, O. *Chem. Rev.* **1992**, *92*, 1007. (c) Narasaka, K. *Synthesis* **1991**, 1.

(13) (a) Markó, I. E.; Evans, G. R.; Seres, P.; Chellé, I.; Janousek, Z. *Pure Appl. Chem.* **1996**, *68*, 113. (b) Evans, D. A.; Murry, J. A.; von Matt, P.; Norcross, R. D.; Miller, S. J. *Angew Chem., Int. Ed. Engl.* **1995**, *34*, 789. (c) Lautens, M.; Tam, W.; Lautens, J. C.; Edwards, L. G.; Crudden, C. M.; Smith, A. C. *J. Am. Chem. Soc.* **1995**, *117*, 6863. (d) Kobayashi, S.; Ishitani, H. *J. Am. Chem. Soc.* **1994**, *116*, 4083. (e) Kündig, E. P.; Bourdin, B.; Bernardinelli, G. *Angew Chem., Int. Ed. Engl.* **1994**, *34*, 1856. (f) Hollis, T. K.; Odenkirk, W.; Robinson, N. P.; Whelan, J.; Bosnich, B. *Tetrahedron* **1993**, *49*, 5415. (g) Davies, D. L.; Fawcett, J.; Garratt, S. A.; Russell, D. R. *J. Chem. Soc., Chem. Commun.* **1997**, 1351. (h) Davenport, A. J.; Davies, D. L.; Fawcett, J.; Garratt, S. A.; Lad, L.; Russell, D. R. *J Chem. Soc., Chem. Commun.* **1997**, 2347. (i) Carmona, D.; Cativiela, C.; Elipe, S.; Lahoz, F. J.; Lamata, M. P.; López-Ram de Víu, M. P.; Oro, L. A.; Vega, C.; Viguri, F. *J. Chem. Soc., Chem. Commun.* **1997**, 2351.

(14) (a) Jimeno, M. L.; Elguero, J.; Carmona, D.; Lamata, M. P.; San José, E. *Magn. Reson. Chem.* **1996**, *34*, 42. (b) Lamata, M. P.; San José, E.; Carmona, D.; Lahoz, F. J.; Atencio, R.; Oro, L. A. *Organometallics* **1996**, *15*, 4852.

(15) White, C.; Yates, A.; Maitlis, P. M. *Inorg. Synth.* **1992**, *29*, 228.

Table 1. ^{1}H NMR Spectroscopic Data[a,b] for Complexes 1−6

complex	C_5Me_5	Me	H_a	H_b	others
1a	1.84 (s)	1.91 (d, J_{HaH} = 7.0)	5.82 (q)	8.95 (d, J_{HaHb} = 1.2)	8.32 (d, J_{HdHc} = 7.7, H_c) 8.26 (td, J_{HeHd} = 7.7, J_{HfHd} = 1.3, H_d) 7.95 (ddd, J_{HfHe} = 5.6, J_{HcHe} = 1.8, H_e) 9.12 (d, H_f), 7.4−7.6 (m, Ph)
1a′	1.84 (s)	2.02 (d, J_{HaH} = 6.8)	5.89 (q)	9.50 (s)	8.37 (d, J_{HdHc} = 7.9, H_c) 9.09 (d, J_{HeHf} = 5.6, H_f) 7.3−8.4 (m, H_{c-e} and Ph)
2a	1.82 (s)	2.09 (d, J_{HaH} = 6.9)	6.41 (q)	9.01 (d, J_{HaHb} = 1.0)	9.19 (d, J_{HeHf} = 5.6, H_f) 7.5−8.3 (m, H_{c-e} and Nph protons)
2a′	1.76 (s)	2.14 (d, J_{HaH} = 6.8)	6.65 (q)	9.72 (s)	9.09 (d, J_{HeHf} = 5.6, H_f) 7.5−8.5 (m, H_{c-e} and Nph protons)
3a	1.72 (s)	2.17 (d, J_{HaH} = 7.0)	6.51 (q)	9.32 (d, J_{HaHb} = 1.5)	7.6−8.8 (m, H_{c-h} and Nph protons)
3a′	1.70 (s)	2.24 (d, J_{HaH} = 7.0)	6.85 (q)	10.15 (s)	7.2−9.9 (m, H_{c-h} and Nph protons)
4a	1.74 (s)	2.06 (d, J_{HaH} = 7.0)	6.30 (q)	9.00 (d, J_{HaHb} = 1.5)	3.20 (s, Me)[c] 7.1−8.4 (m, H_{c-e} and Nph protons)
4a′	1.72 (s)	2.17 (d, J_{HaH} = 7.0)	6.72 (q)	9.89 (s)	3.12 (s, Me)[c] 7.1−8.4 (m, H_{c-e} and Nph protons)
5a	1.78 (s)	1.50 (d, J_{HaH} = 6.6)	4.24 (q)	9.46 (s)	8.38 (d, J_{HdHc} = 7.8, H_c) 8.31 (td, J_{HeHd} = 7.8, J_{HfHd} = 1.3, H_d) 7.95 (m, J_{HfHe} = 5.6, J_{HcHe} = 1.6, H_e) 9.11 (d, H_f), 1.2−2.2 (m, Cy)
5a′	1.81 (s)	1.56 (d, J_{HaH} = 6.8)	4.63 (q)	9.27 (d, J_{HaHb} = 1.2)	8.42 (d, J_{HdHc} = 7.7, H_c) 8.33 (td, J_{HeHd} = 7.7, J_{HfHd} = 1.3, H_d) 7.95 (m, J_{HfHe} = 5.6, J_{HcHe} = 1.6, H_e) 9.06 (d, H_f), 1.0−2.4 (m, Cy)
6a	1.75 (s)	-	5.07 (q)	9.34 (s)	8.51 (d, J_{HdHc} = 7.8, H_c) 7.90 (m, H_d), 7.28 (m, H_e) 8.97 (d, J_{HeHf} = 5.1, H_f) 0.98 (s),[d] 1.15 (s),[d] 1.20 (s)[d] 1.5−3.0 (m)[e]
6a′	1.74 (s)		4.67 (q)	9.28 (d, J_{HaHb} = 2.4)	8.51 (d, J_{HdHc} = 7.8, H_c) 7.90 (m, H_d), 7.28 (m, H_e) 9.02 (d, J_{HeHf} = 5.4, H_f) 0.93 (s),[d] 1.08 (s),[d] 1.30 (s)[d] 1.5−3.0 (m)[e]

[a] Measured in $(CD_3)_2CO$. Chemical shifts in ppm with TMS an external standard. Coupling constants in Hertz. Abbreviations: s, singlet; d, doublet; dt, doublet of triplets; q, quartet; m, multiplet. [b] For proton labeling, see Scheme 1. [c] Me of pyridinic ring. [d] Me groups of the bornyl substituent. [e] Remaining bornyl protons.

the stereogenic iridium center (eq 1). A single recrys-

$$^1/_2[\{(\eta^5\text{-}C_5Me_5)IrCl\}_2(\mu\text{-}Cl)_2] + L_n + NaSbF_6 \rightarrow [(\eta^5\text{-}C_5Me_5)IrCl(L_n)][SbF_6] + NaCl \quad (1)$$

L_1: **1a**:**1a′**, 78:22 L_4: **4a**:**4a′**, 80:20

L_2: **2a**:**2a′**, 61:39 L_5: **5a**:**5a′**, 43:57

L_3: **3a**:**3a′**, 72:28 L_6; **6a**:**6a′**, 52:48

tallization from diethyl ether was sufficient to obtain diastereomers **1a**−**5a** in essentially complete optical purity (>98% by ^{1}H NMR), and mixtures enriched in the **a′** diastereomer were also isolated from the mother liquors for compounds **1** (**1a**:**1a′**, 32:68), **3** (**3a**:**3a′**, 17:83), and **5** (**5a**:**5a′**, 19:81). The isomer ratio was obtained from accurate integration[16] of the H_a or the deshielded imino H_b proton signals of each diastereomer (Scheme 1). Complexes **1**−**6** have been characterized by analytical and spectroscopic means and by crystal structure determination by X-ray diffractometric methods for compounds **1a**, **2a**, and **3a**. Their IR spectra showed a ν(C═N) band at ca. 1600 cm^{-1}. Table 1 collects the ^{1}H NMR data for these complexes. In some cases, the assignments have been completed on the basis of NOE and 2D ^{1}H−^{1}H correlation spectra. In all cases, the spectral data were consistent with the presence of the η^5-C_5Me_5 and pyridine−imine ligands in a 1:1 ratio. The chemical shift of the H_b protons appeared at significantly higher field for compounds **1a**−**4a** than for the corresponding **1a′**−**4a′** isomers, but it did not differ appreciably between **5a**, **6a** and the corresponding **5a′**, **6a′** compounds. Most probably, the asymmetric carbon atom of complexes **1a**−**4a** adopts such a conformation in solution that the smallest sized H_a hydrogen points toward the bulkiest C_5Me_5 group and the R substituent roughly eclipses the N_{im}−C(H_b) bond (see Figure 1a). In this conformation, the H_b hydrogens are subject to a ring current effect from the aromatic R substituents (phenyl (**1a**) or naphthyl (**2a**−**4a**)) that originates the high-field shift found (Figure 1c). On the other hand, the conformation around the asymmetric carbon atom in the **a′** diastereomers **1a′**−**4a′** would retain the H_a atom pointing toward the C_5Me_5 group, but the change of configuration at the iridium now forces the methyl to approximately eclipse the N_{im}−C(H_b) bond. Consequently, the shielding of the H_b protons by the R groups is now precluded (Figure 1b). Obviously, this effect does not operate in the cases of the cyclohexyl (**5**) or bornyl (**6**) substituents, and their H_b protons resonate at similar frequencies in both isomers. The particular

(16) Solid samples of different compositions can be prepared by recrystallization from different solvents. Thus, for example, the orange solid (brown for complex **3**) which spontaneously precipitates in the preparation of the complexes (see Experimental Section) has the following **a**:**a′** composition (molar ratio): **1**, >98:<2; **2**, 48:52; **3**, >98:<2; **4**, >98:<2; **5**, >98:<2; **6**, 50:50. Error limits on each integer are estimated as ±2.

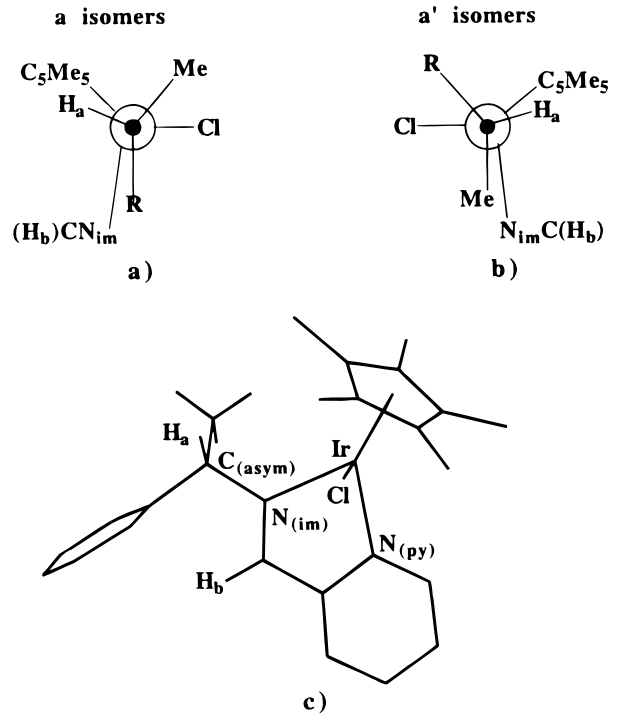

Figure 1. Schematic projections along the C(asymmetric)−Ir direction of the proposed molecular structure in solution for (a) **a** isomers; (b) **a′** isomers. (c) Molecular model for isomer **1a** showing the proposed relative disposition in solution of Ph and H_b.

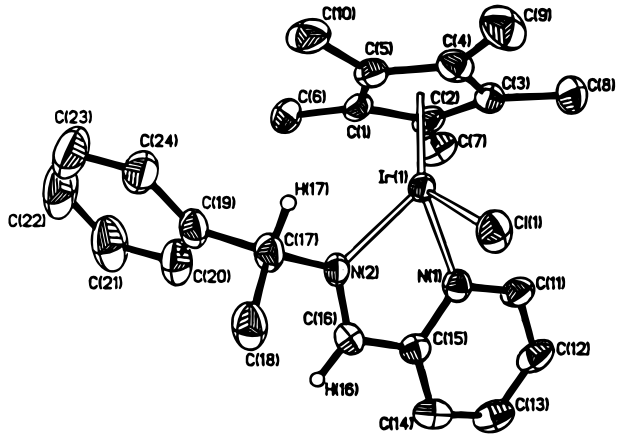

Figure 2. Molecular view of the cation of the complex [(η^5-C_5Me_5)IrCl(L_1)][SbF_6] (**1a**).

intramolecular interactions present in these two conformations between the chiral auxiliary and the remaining portion of the molecule seem to play a major role in the relative stabilities of the (*R*)- and (*S*)-metalloepimers (vide infra).

Molecular Structure of the Diastereomers 1a, 2a, and 3a. To determine the absolute configuration of the chloro−imino compounds, the molecular structures of **1a**, **2a**, and **3a** were elucidated by diffractometric means. Single crystals of the complexes were grown by slow diffusion of petroleum ether into methanol (**1a**), chloroform (**2a**), or acetone−methanol (**3a**) solutions. Molecular representations of the cations of complexes **1a**, **2a**, and **3a** are depicted in Figures 2, 3, and 4 and selected structural parameters are listed in Table 2. All three cations exhibit "three-legged pianostool" geometries. An η^5-C_5Me_5 group occupies three *fac*

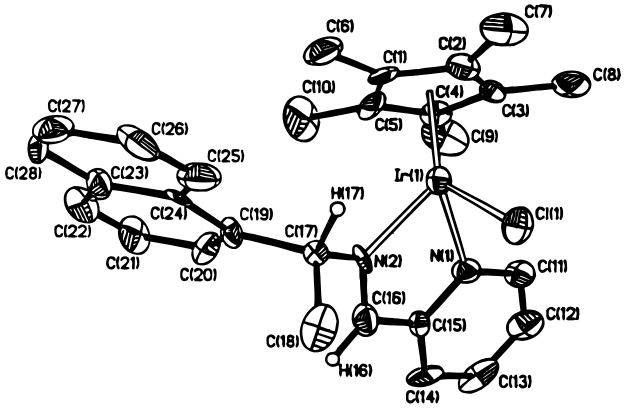

Figure 3. Molecular view of the cation of the complex [(η^5-C_5Me_5)IrCl(L_2)][SbF_6] (**2a**).

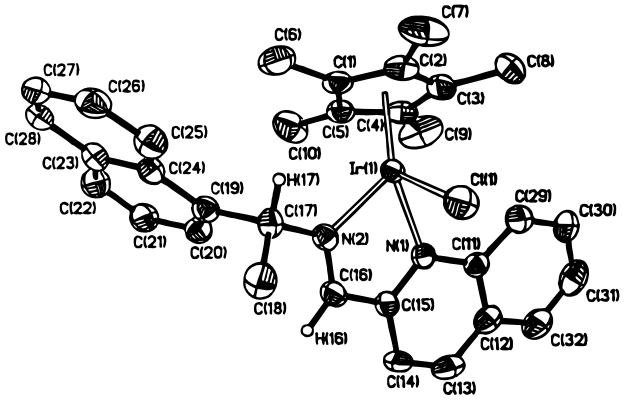

Figure 4. Molecular view of the cation of the complex [(η^5-C_5Me_5)IrCl(L_3)][SbF_6] (**3a**).

positions, and the chelating pyridine−imine ligand and one chlorine atom complete the coordination sphere of the metal. In general, no significant differences are observed in the bond lengths and angles of the three structures. Only some of the bonding parameters involving the pyridinic nitrogen N(1) in **3a**, such as the Ir(1)−N(1), N(1)−C(11), and N(1)−C(15) distances and the Cl(1)−Ir(1)−N(1) and N(1)−Ir(1)−G(1) angles, are slightly different from those corresponding to **1a** or **2a**, most probably reflecting the presence of the geometrically constrained quinolyl residue in that compound. The absolute configuration of the iridium center in the three complexes is *R* according with the ligand priority sequence[17] η^5-C_5Me_5 > Cl > N(im) > N(py). In the three structures, the Ir(1)−N(1)−C(15)−C(16)−N(2) metallacycle is essentially planar. Strikingly, in the solid-state molecular structure of these complexes, the H_b protons do not lie in the shielding cone of the phenyl or naphthyl substituents. To account for the reported ^{1}H NMR data, rotations around the N(2)−C(17) and the C(17)−C(19) single bonds have to be proposed when going from the solid state to solution. A rotation around the N(2)−C(17) bond reducing the torsion angle C(16)−N(2)−C(17)−C(19) from the value observed in the solid state (for example, −94.6° in **1a**) to values close to 0° is necessary to bring the phenyl or naphthyl groups to the

(17) (a) Cahn, R. S.; Ingold, C.; Prelog, V. *Angew. Chem, Int. Ed. Engl.* **1966**, *5*, 385. (b) Lecomte, C.; Dusausoy, Y.; Protas, J.; Tirouflet, J. *J. Organomet. Chem.* **1974**, *73*, 67. (c) Stanley, K.; Baird, M. C. *J. Am. Chem. Soc.* **1975**, *97*, 6599. (d) Sloan, T. E. *Top. Stereochem.* **1981**, *12*, 1.

Table 2. Selected Bond Distances (Å) and Angles (deg) for Complexes 1a, 2a, and 3a

	1a	2a	3a
Ir−Cl	2.3845(13)	2.392(4)	2.3858(14)
Ir−N(1)	2.076(4)	2.092(11)	2.124(4)
Ir−N(2)	2.105(4)	2.059(12)	2.096(4)
Ir−C(1)	2.161(4)	2.216(18)	2.186(5)
Ir−C(2)	2.167(4)	2.15(2)	2.182(5)
Ir−C(3)	2.153(5)	2.10(2)	2.191(5)
Ir−C(4)	2.180(5)	2.149(14)	2.185(5)
Ir−C(5)	2.171(5)	2.172(19)	2.159(5)
Ir-G[a]	1.793(4)	1.788(14)	1.815(6)
N(1)−C(11)	1.336(6)	1.322(19)	1.373(6)
N(1)−C(15)	1.360(6)	1.370(18)	1.335(6)
C(15)−C(16)	1.459(7)	1.47(2)	1.446(7)
C(16)−N(2)	1.277(6)	1.29(2)	1.284(7)
N(2)−C(17)	1.486(6)	1.502(17)	1.481(7)
C(17)−C(18)	1.533(7)	1.53(2)	1.524(7)
C(17)−C(19)	1.526(7)	1.548(19)	1.533(7)
Cl−Ir−N(1)	87.52(12)	88.1(4)	83.82(12)
Cl−Ir−N(2)	81.91(12)	84.0(3)	84.96(11)
Cl−Ir-G[a]	125.64(11)	124.5(5)	126.1(2)
N(1)−Ir-N(2)	76.53(16)	76.4(5)	76.3(2)
N(1)−Ir-G[a]	130.5(2)	129.9(7)	134.2(2)
N(2)−Ir-G[a]	136.4(2)	136.5(7)	132.6(3)
Ir−N(1)−C(11)	126.2(3)	125.4(11)	127.1(3)
Ir−N(1)−C(15)	116.4(3)	115.7(10)	114.8(3)
N(1)−C(15)-C(14)	122.9(5)	122.6(14)	123.5(5)
N(1)−C(15)-C(16)	113.1(4)	110.9(13)	114.8(4)
C(15)−C(16)-N(2)	117.7(4)	117.4(14)	117.7(5)
Ir−N(2)−C(16)	116.1(3)	117.2(10)	116.2(4)
Ir−N(2)−C(17)	122.5(3)	122.8(10)	123.9(3)
C(16)−N(2)-C(17)	120.5(4)	118.5(13)	119.7(4)

[a] G represents the centroid of the pentamethylcyclopentadienyl ring.

proximity of the H_b proton. An additional rotation of these groups around the C(17)−C(19) bond (ca. 54° in **1a**) is required to properly orientate the electronic π current of the rings to affect the H_b NMR signal. Interestingly, one of the two independent molecules found in the solid-state structure of the related mesytilene ruthenium compound (S_{Ru},S_C)-[(η^6-mes)RuCl(imine)]BF_4 (imine = *N*-(2-pyridylmethylene)-(*S*)-1-phenylethylamine) has a conformation in which the phenyl substituent is almost eclipsed and face-on to the imine nitrogen[6i] in a very similar situation to that described for **1a**−**4a** in solution. However, no evident intra- or intermolecular interactions have been detected to account for these facts.

Circular Dichroism Spectra. Diastereomeric pure samples of complexes **1a**−**3a** (R_{Ir} epimers) have a negative Cotton effect at ca. 450 nm in their CD spectra. The CD spectra of pure **4a** and **5a** or of a 92:8 **a**:**a′** mixture of **6** also show a negative Cotton effect centered at about 450 nm. Complexes **1a**, **2a**, **4a**, and **6a** also have positive (at ca. 325 nm) and negative (at ca. 360 nm) maxima. The CD spectrum of complex **1a** also contains a transition at 395 nm, and the **2a** maximum at 360 nm has a shoulder at 380 nm. As expected for epimers differing in the metal configuration,[1c,4c] **a** and **a′** pairs exhibit CD spectra that are approximately mirror images of each other, showing that the major contribution to the spectra corresponds to the metal chromophore. As representative examples, Figures 5 and 6 show the pseudo-enantiomorphic relationship between **3a** and **5a** and enriched mixtures in their respective **3a′** and **5a′** epimers. All of the spectral data taken together with the above-reported diffractometric

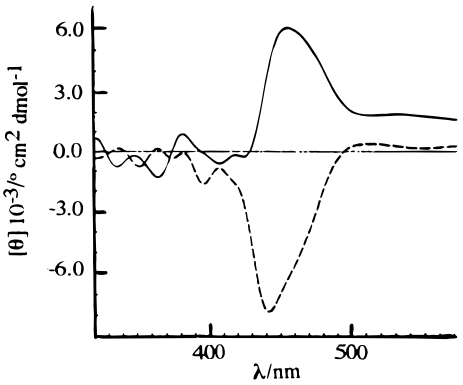

Figure 5. CD spectra (Me_2CO, 1.25 × 10^{-3} mol L^{-1}) of complex **3a** (- - -) and of a 17:83 **3a**:**3a′** mixture (—).

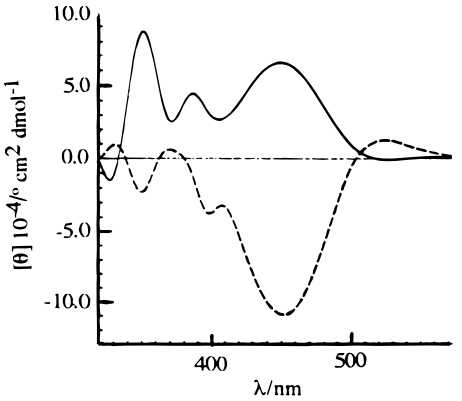

Figure 6. CD spectra (Me_2CO, 1.25 × 10^{-3} mol L^{-1}) of complex **5a** (- - -) and a 20:80 **5a**:**5a′** mixture (—).

Table 3. Diastereomeric Compositions of Complexes 1−6

complex	initial **a**:**a′** molar ratio	equilibrium **a**:**a′** molar ratio
1	56:44	82:18
2	43:57	90:10
3	17:83	90:10
4	56:44	87:13
5	>98:<2	19:81
6	50:50	92:8

results allows us to propose the R_{Ir} and S_{Ir} configurations for the **a** and **a′** isomers, respectively.

Epimerization of the Complexes 1−6. At room temperature, in acetone solution, the iridium center in complexes **1**−**6** is configurationally stable: solution mixtures of **a** and **a′** isomers remained unchanged for 24 h. Thus, conversely to the amino acidato ligand in [(η^5-C_5Me_5)Ir(α-amino acidato)L] systems,[5e,j,k] the pyridine−imine ligands confer a remarkable configurational stability at the iridium center in the [(η^5-C_5Me_5)IrCl(L_n)][SbF_6] compounds. However, at higher temperatures in more polar solvents such as methanol, the complexes slowly epimerize at iridium without apparent decomposition. Table 3 collects the initial diastereomeric compositions[16] and those at the equilibrium reached after about 30 h of treatment in refluxing methanol. The latter composition remained unchanged after refluxing the mixtures for 8 additional hours.

For reasons of rate convenience, the epimerization of complex **5a** was monitored by ^{1}H NMR spectroscopy in methanol-d_4 at 45, 49, 55, 59, and 62 °C. Integration of the imino proton H_b resonances at ca. 9.2 and 9.4 ppm, assignable to the (*S*)- and (*R*)-epimers, respec-

tively, affords kinetic data. In all cases, the epimerization turned out to be a clean first-order reaction with k' values ranging from 2.7×10^{-5} to 1.7×10^{-4} s^{-1}. The half-life of the approach to the equilibrium at 62 °C was 68.0 min. Activation parameters for the **5a** ⇌ **5a′** process were calculated on the basis of the exchange rates at different temperatures. These are $\Delta H^{\ddagger} = 97.7 \pm 13.2$ kJ mol^{-1} and $\Delta S^{\ddagger} = -26.3 \pm 6.2$ J K^{-1} mol^{-1}. Moreover, the isomerization process was carried out at 60 °C in the same conditions as above but in the presence of an excess (from 6.2 to 15.3-fold) of the cyclohexylimine ligand L_5 and at 62 °C in the presence of Cl^- (from 6.0 to 15.2-fold excess). The rate of epimerization hardly varied in the first case and slightly increased (from 1.7 to 2.5-fold) when the chloride concentration increased, probably due to the concomitant increase of the ionic strength of the solution. Furthermore, we have refluxed together equimolar amounts of **5a** and the rhodium analogue $[(\eta^5\text{-}C_5Me_5)\text{-}RhCl(L_2)][SbF_6]$ in methanol for 2 h. In these conditions both complexes epimerized at the metal.[18] Neither the iridium complexes **2** nor the cyclohexylimine rhodium complex $[(\eta^5\text{-}C_5Me_5)RhCl(L_5)]^+$ have been detected by NMR spectroscopy.

On the other hand, from 45 to 62 °C, the equilibrium constant for the interconversion **5a** ⇌ **5a′** is 4.26 ± 1.65 and exhibits a negligible temperature dependence within experimental error. From the van't Hoff equation, values of $\Delta H \approx 0$ kJ mol^{-1} and $\Delta S \approx 12$ J K^{-1} mol^{-1} have been obtained, indicating that the two epimers have similar bonding energetics and steric interactions.

All of these data strongly suggested a dissociative mechanism involving an intermolecular halogen exchange for the epimerization process. This would be favored by a polar solvent, which would stabilize the 16-electron two-legged piano-stool intermediate $[(\eta^5\text{-}C_5Me_5)Ir(L_n)]^{2+}$. This intermediate could be planar or pyramidal.[19] Chloride attack to the opposite side if the intermediate is planar[5m] or after inversion if pyramidal leads to epimerization at metal.

The diastereomeric equilibrium ratios, collected in Table 3, deserve some further comments. The thermodynamically more stable diastereomer is the **a** epimer (R_{Ir}) for complexes **1**−**4** and **6** but the **a′** epimer (S_{Ir}) for complex **5**. Figure 1 shows schematically the projection of the **a** and **a′** isomers along the C(17)−Ir(1) direction, which agrees with the discussed ^1H NMR data. Assuming the H_a proton pointing to the C_5Me_5 group in both diastereomers, the R substituents and the essentially planar IrNCCN metallacycles (represented in Figure 1 by the $N_{im}C(H_b)$ group) should be in almost eclipsing positions. This conformation is favored with respect to that adopted by the **a′** isomers (obtained interchanging the relative positions of the Me and R groups) when R is the planar phenyl or naphthyl substituent (**1**−**4**) as well as for the bornyl group of complex **6**. However, when R is the nonplanar cyclohexyl group (**5**), there would be an important repulsive interaction between the closer axial protons of this cycle and the $N_{im}C(H_b)$ moiety that favors the **a′** conformation showed in Figure 1b. Support for this latter proposal stems from the observed strong NOE[20] for the cyclohexyl group (12.2%) when the H_b proton was irradiated, in isomer **5a**, while any enhancement in the cyclohexyl signals of the **5a′** isomer when the corresponding H_b proton was saturated was not observed. Furthermore, irradiation of the H_b proton produces a greater enhancement at the Me of the chiral imine in **5a′** (5.8%) than in **5a** (2.1%) (see Experimental Section).

Diastereomeric Complexes $[(\eta^5\text{-}C_5Me_5)IrCl(L_2)]A$ (7−10). One of the aims of this work was to explore the ability of the new chiral imino complexes as catalyst precursors for enantioselective Diels−Alder reactions. Evans et al. have very recently reported that the catalytic efficiency of bis(oxazolinyl) Cu(II) complexes in the cycloaddition of methacrolein with cyclopentadiene is largely affected by changing the noncoordinating counterion from $CF_3SO_3^-$ to SbF_6^-, PF_6^-, or BF_4^-.[13b] For this reason we envisaged the preparation of a series of complexes $[(\eta^5\text{-}C_5Me_5)IrCl(L_2)]A$ in which the cation of complex **2** crystallizes with different anions (A = Cl (**7**), BF_4 (**8**), PF_6 (**9**), (*1S*)-camphor-10-sulfonate (R^*SO_3) (**10**)).

The chloride complex **7** was prepared according to eq 2 as a, 70:30 **7a**:**7a′** mixture of epimers at metal.

$$^1/_2[\{(\eta^5\text{-}C_5Me_5)IrCl\}_2(\mu\text{-}Cl)_2] + L_2 \rightarrow \underset{\mathbf{7}}{[(\eta^5\text{-}C_5Me_5)IrCl(L_2)]Cl} \quad (2)$$

Diastereomeric mixtures of the complexes **8**−**10** (**8a**:**8a′**, 62:38; **9a**:**9a′**, 66:34; **10a**:**10a′**, 90:10) can be prepared by adding, in methanol, equimolar amounts of $NaBF_4$, $NaPF_6$, or HR^*SO_3 and KOH, respectively, to 70:30 mixtures of the chloride **7**. Recrystallization of **8** and **9** from methanol/diethyl ether afforded 70:30 **8a**:**8a′** and 80:20 **9a**:**9a′** molar ratio mixtures. The new complexes have been characterized by elemental analysis[21] and spectroscopic methods (see Experimental Section). As observed for complex **2**, the H_b resonance of the major **a** isomers appears 0.53−0.83 ppm shifted to higher field with respect to the corresponding **a′** signal. The CD traces of the mixtures enriched in the **a** component compare well with that of complex **2a**, which has been characterized by X-ray analysis as the *R* isomer at the iridium. All of these data are compatible with an *R* configuration at iridium for the major **7a**−**10a** epimers.

Solvated Complexes $[(\eta^5\text{-}C_5Me_5)Ir(L_6)(H_2O)][SbF_6]_2$ (11a,a′). Preliminary studies showed that the chloride compounds **1**−**10** were not active as catalysts for the Diels−Alder reaction. Most probably the coordinative saturation of the metallic center in these complexes avoids catalysis. To get complexes with a vacant or more labile ligand in the metal sphere, we treated the chloride compounds **1**−**10** with silver salts as halogen scavengers. The resulting mixtures were not stable enough to be studied by spectroscopic means, except in the case of the bornylimine derivative **6**. Thus, acetone-d_6 solutions of 85:15 diastereomeric mixtures

(18) The rhodium complex $[(\eta^5\text{-}C_5Me_5)RhCl(L_2)][SbF_6]$ was prepared as described for the related iridium analogues **1**−**6** and epimerizes at rhodium in refluxing methanol: Carmona, D.; Lahoz, F. J.; Elipe, S.; Oro, L. A.; Lamata, M. P.; Viguri, F.; García-Correas, R.; Vega, C.; Cativiela, C.; López-Ram de Víu, M. P. Unpublished results.

(19) Ward, T. R.; Schafer, O.; Daul, C.; Hofmann, P. *Organometallics* **1997**, *16*, 3207 and references therein.

(20) Neuhaus, D.; Williamson, M. *The Nuclear Overhauser Effect in Structural and Conformational Analyses*; VCH: New York, 1989.

(21) Complexes **7**, **8**, and **10** contained variable amounts of water of crystallization, as inferred from their IR spectra.

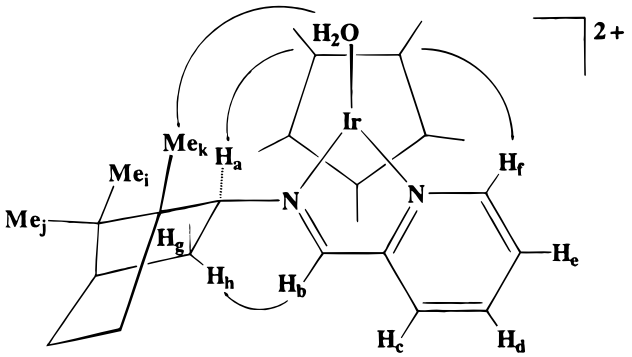

Figure 7. Schematic view of the cation $[(\eta^5\text{-}C_5Me_5)(L_6)(H_2O)]^{2+}$ (**11a**). Proton labeling and some selected NOE are shown.

of the new complex $[(\eta^5\text{-}C_5Me_5)Ir(L_6)(H_2O)][SbF_6]_2$ were prepared by treating 50:50 mixtures of the chloro compound **6** with equimolar amounts of $AgSbF_6$ in the presence of water and subsequent separation of the AgCl formed. The assignment of the NMR resonances of the aquo diastereomers (see Experimental Section) are based on NOE and on 2D $^1H-^1H$ correlation spectroscopic measurements. Besides the expected resonances for the protons of the C_5Me_5 and L_6 groups, the ^1H NMR spectrum showed peaks of coordinated and free water that, at room temperature, independently appeared at 7.65 and 3.00 ppm,[22] respectively, for the major diastereomer. ROESY experiments indicated that slow exchange processes were occurring between the coordinated and free water and also between the two isomeric aquo complexes. The CD spectrum in acetone of a 85:15 mixture of the aquo complexes **11** closely resembles that found for a 92:8 **6a**:**6a′** mixture: a negative Cotton effect at ca. 450 nm is the dominant feature in both spectra. NOE difference spectra[20] (see Figure 7) showed that irradiation of the C_5Me_5 protons led to enhancement of the H_f (0.5%) and the bornyl H_a (0.4%) protons, irradiation of the H_b proton causes an enhancement of the H_h proton (9.6%), and irradiation of the coordinated water singlet produced an enhancement of the bornyl methyl Me_k (4.0%). Taken together, these data strongly support an *R* configuration at Ir for the major diastereomer of the aquo complex $[(\eta^5\text{-}C_5Me_5)Ir(L_6)(H_2O)][SbF_6]_2$, as well as a conformation similar to that depicted in Figure 1 for the **a** isomers.

Catalytic Diels−Alder Reactions. Solvate complexes $[(\eta^5\text{-}C_5Me_5)Ir(imine)S]^{2+}$ prepared in situ by treating the corresponding chloride compounds **1**−**6** with $AgSbF_6$ are active catalysts for the Diels−Alder reaction between methacrolein and cyclopentadiene. Table 4 summarizes the most representative results. A 5:100 precatalyst:methacrolein and 6:1 cyclopentadiene:methacrolein molar ratio was used in all cases. Enantioselectivities up to 46% were achieved, and as expected, better exo:endo and enantioselectivities were obtained at lower temperatures for all of the six imine ligands. Similar results have been obtained when using precatalysts differing in their epimeric composition at the metal (compare entries 2 with 3 or 12 with 13). Most probably, the catalytic processes include epimerization

Table 4. Enantioselective Diels−Alder Reaction of Methacrolein with Cyclopentadiene Catalyzed by Complexes 1−6 and 8−10 in Dichloromethane-acetone

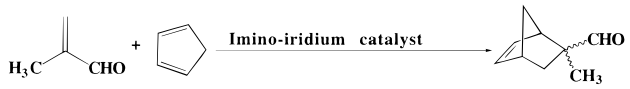

entry	precatalyst (**a**:**a′**, ratio)	temp (C)	time (h)	yield (%)	isomer ratio (exo:endo)	ee[a] (%)
1		RT	1	0.5		
2	**1** (32:68)	RT	0.9	91	90:10	7 (*S*)
3	**1** (>98:<2)	RT	1.5	94	90:10	5 (*S*)
4	**1** (>98:<2)	−50	94	48	93:7	32 (*S*)
5	**2** (>98:<2)	RT	1.6	89	90:10	14 (*S*)
6	**2** (>98:<2)	−50	96	21	94:6	46 (*S*)
7	**3** (>98:<2)	RT	2	94	85:15	0
8	**3** (>98:<2)	−50	144	29	88:12	20 (*R*)
9	**4** (47:53)	RT	2.5	71	89:11	0
10	**4** (47:53)	−20	72	74	87:13	6 (*R*)
11	**5** (>98:<2)	−20	16	65	94:6	30 (*R*)
12	**5** (>98:<2)	−50	24	28	95:5	34 (*R*)
13	**5** (20:80)	−50	46	31	95:5	22 (*R*)
14	**6** (50:50)	RT	0.3	100	90:10	20 (*S*)
15	**6** (50:50)	−50	72	58	93:7	38 (*S*)
16	**8** (70:30)	RT	4	78	85:15	0
17	**9** (80:20)	RT	15	81	84:16	0
18	**10** (90:10)	RT	23	28	85:15	0

[a] Absolute configuration at C_2.

steps that account for these results. Furthermore, when complexes **8**−**10** (which contain the same imino−iridium cation as **2**) were used as catalyst precursors (entries 16−18), rates and selectivities decreased with respect to those obtained with **2**. Consequently, we have not performed further studies with these precatalysts.

The preferential adduct obtained with precatalysts **1**, **2**, and **6** was (1*R*,2*S*,4*R*)-2-methylbicyclo[2.2.1]hept-5-ene-2-carbaldehyde, whereas the (1*S*,2*R*,4*S*) enantiomer was the predominant adduct with **3**, **4**, and **5**. It is generally accepted that the transition-metal Lewis acid catalytic formation of Diels−Alder adducts includes the interaction between the Lewis acid−dienophile complex and the diene.[9b,13,23] The proposed conformations for the **a** and **a′** chloride epimers (Figure 1) would account for the preferential *S* configuration at C_2 for the Diels−Alder adduct with the **1**, **2**, and **6** precatalysts (epimer **a** more stable) as well as for the ee in the *R* at C_2 for the adduct with **5** (epimer **a′** more stable). If the Lewis acid−dienophile adduct has the conformation of the **a** isomers and the methacrolein adopts the s-trans preferred disposition,[13i] the si-face of the dienophile is shielded by the methyl group of the chiral imine. The attack of the diene would take place preferentially on the re-face and ee would be achieved in the (1*R*,2*S*,4*R*) configurated adduct (Figure 8a). Conversely, in the Lewis acid−dienophile adducts with an **a′** conformation, the attack of the diene would predominantly occur on the si-face because the R group is now shielding the re-face of the dienophile. The favored adduct would be the (1*S*,2*R*,4*S*) enantiomer (Figure 8b).

To account for the enantioselectivity observed for the **3a** and **4a** precatalysts (*R* at C_2 enantiomer was

(22) A chemical shift of 6.60 ppm has been recently reported for coordinated water in a related pseudo-octahedral $(C_6H_6)Ru$ aquo complex, See: Asano, H.; Katayama, F.; Kurosawa, H. *Inorg. Chem.* **1996**, *35*, 5760.

(23) In fact, we have recently reported the X-ray molecular structure of the ruthenium Lewis acid−dienophile adduct (S_{Ru})-$[(\eta^6\text{-}p\text{-cymene})Ru(PN)(methacrolein)][SbF_6]_2$ and showed that it is involved in the Diels−Alder reaction between methacrolein and cyclopentadiene.[13i]

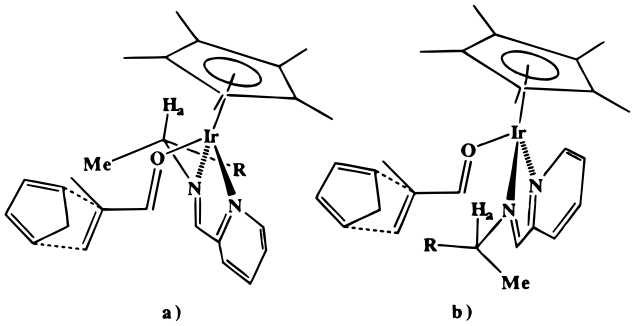

Figure 8. Schematic view of the proposed transition state for the Diels−Alder catalytic reactions: (a) **a** and (b) **a′** isomers.

preferred), it is interesting to note the perceivable changes detected in the molecular structure of **3a** involve the parameters around the quinolyl nitrogen atom (see above). These structural changes, if retained in the Lewis acid−dienophile adducts derived from **3a** and **4a**, would bring the C_5Me_5 ligand slightly toward the coordinated methacrolein, shielding its re-face. The steric hindrance on this face would be greater than that produced on the opposite face by the Me of the chiral imine and would account for the observed results.

Concluding Remarks

In this paper it has been shown that the conformation around the chiral imine center determines the relative stability of the two possible epimers at the metal in the new imino−iridium(III) compounds **1**−**6** and allows one to predict the direction of the observed epimerization processes. Interestingly, significant conformational differences have been observed between the molecular structures of the solids **1a**−**3a** and their solutions. Compounds **1**−**6** are active catalyst precursors for the Diels−Alder reaction between methacrolein and cyclopentadiene. The observed enantioselectivities could be understood on the basis of the conformation adopted by the imine chiral carbon atom in each epimer at metal. Finally, it has been possible to study the in situ formation of the aquo-solvate **11** from the chloride complex **6**. This solvate or, in general, solvate complexes related to **11** could be considered as the actual catalysts in the aforementioned Diels−Alder process.

Experimental Section

General Comments. All solvents were dried over appropriate drying agents, distilled under nitrogen, and degassed prior to being used. All preparations have been carried out under a nitrogen atmosphere. Infrared spectra were recorded on a Perkin-Elmer 783 spectrophotometer. Carbon, hydrogen, and nitrogen analyses were performed using a Perkin-Elmer 240B microanalyzer. ^{1}H NMR spectra were recorded on a Varian UNITY 300 (299.95 MHz) and a Bruker 300 ARX (300.10 MHz). Chemical shifts are expressed in ppm upfield from $SiMe_4$. The probe temperature was calibrated against a methanol standard. COSY and NOEDIFF spectra were obtained using standard procedures. The ROESY spectrum was obtained for a spin-locking (mixing) time of 400 ms. CD spectra were determined in Me_2CO (ca. 10^{-3} mol L^{-1} solutions) in a 1-cm path length cell by using a Jasco-710 apparatus.

Preparation of [(η^5-C_5Me_5)IrCl(imine)][SbF_6] (1−6). A mixture of [{(η^5-C_5Me_5)IrCl}$_2$(μ-Cl)$_2$] (200.0 mg, 0.251 mmol), $NaSbF_6$ (130.0 mg, 0.502 mmol), and the appropriate imine ligand (0.502 mmol) in methanol (25 mL) was stirred for 2 h. During this time, the precipitation of an orange (brown for complex **3**) solid was observed.[16] The resulting suspension was vacuum-evaporated to dryness. The residue was extracted with dichloromethane (15 mL), and the solution was partially concentrated under reduced pressure. Slow addition of diethyl ether gave an orange microcrystalline solid (brown for complex **3**), which was filtered off, washed with diethyl ether, and air-dried. By recrystallization from methanol−diethyl ether, pure **1a**−**5a** and mixtures of molar compositions 32:68 **1a**:**1a′**, 48:52 **2a**:**2a′**, 17:88 **3a**:**3a′**, 56:44 **4a**:**4a′**, 19:81 **5a**:**5a′**, and 64:36 **6a**:**6a′** were obtained. Complex **1**. Yield: 84%. Anal. Calcd for $C_{24}H_{29}N_2ClF_6IrSb$: C, 35.63; H 3.61; N, 3.46. Found: C, 35.45; H 3.15; N, 3.36. IR (Nujol, cm^{-1}): ν(CN) 1595 (s), ν-(SbF_6) 285 (s). Complex **1a**. Selected NOE data (irradiated nucleus(i); enhanced protons (%)). H_a: H_b (0.9), C_5Me_5 (9.0), Ph (5.8), Me (4.4). H_b: H_c (13.8), Ph (6.3). H_f: H_e (8.3), C_5-Me_5 (9.0). C_5Me_5: H_f (0.4), H_b (0.7), Ph (1.4), H_a (2.2). Me: H_f (0.7), H_b (1.0), Ph (2.1), H_a (2.5). Complex **1a′**. Selected NOE data (irradiated nucleus(i); enhanced protons (%)). H_b: H_c (6.85). C_5Me_5: H_f (0.2), H_a (0.25). Me: H_b (0.1), H_f (0.1), H_a (0.5). Complex **2**. Yield: 88%. Anal. Calcd for $C_{28}H_{31}N_2ClF_6IrSb$: C, 39.15; H, 3.63; N, 3.26. Found: C, 38.88; H, 3.60; N, 3.24. IR (Nujol, cm^{-1}): ν(CN) 1595 (s), ν(SbF_6) 285 (s). Complex **3**. Yield: 80%. Anal. Calcd for $C_{32}H_{33}N_2ClF_6$-IrSb: C, 42.28; H, 3.66; N, 3.08. Found: C, 42.07; H, 3.83; N, 2.77. IR (Nujol, cm^{-1}): ν(CN) 1595 (s), ν(SbF_6) 290 (s). Complex **4**. Yield: 93%. Anal. Calcd for $C_{29}H_{33}N_2ClF_6IrSb$: C, 39.89; H, 3.81; N, 3.20. Found: C, 39.66; H, 3.40; N, 3.02. IR (Nujol, cm^{-1}): ν(CN) 1600 (s), ν(SbF_6) 290 (s). Complex **5**. Yield: 83%. Anal. Calcd for $C_{24}H_{35}N_2ClF_6IrSb$: C, 35.37; H, 4.32; N, 3.43. Found: C, 34.91; H, 4.14; N, 3.36. IR (Nujol, cm^{-1}): ν(CN) 1595 (s), ν(SbF_6) 285 (s). Complex **5a**. Selected ^{1}H−^{1}H COSY data: H_f correlated with H_e. Selected NOE data (irradiated nucleus(i); enhanced protons (%)). Ha: C_5Me_5 (6.1), Me (0.2). H_b: H_c (7.2), Cy (12.2), C_5Me_5 (4.2), Me (2.1). H_f: He (7.5), C_5Me_5 (8.2). C_5Me_5: H_b (0.1), H_f (0.7), H_a (0.6). Me: H_b (1.05), H_a (3.4). Complex **5a′**. Selected NOE data (irradiated nucleus(i); enhanced protons (%)). H_a: Cy (6.3), C_5Me_5 (16.8), Me (5.6). H_b: H_c (4.5), C_5Me_5 (2.6), Me (5.8). H_f: H_e (5.0), C_5Me_5 (6.8), Me (1.7). C_5Me_5: H_f (0.95), H_a (1.4). Me: H_b (3.0), H_a (2.2). Complex **6**. Yield: 87%. Anal. Calcd for $C_{26}H_{37}N_2ClF_6IrSb$: C, 37.13; H, 4.43; N, 3.33. Found: C, 36.67; H 4.22; N, 3.21. IR (Nujol, cm^{-1}): ν(CN) 1595 (s), ν(SbF_6) 285 (s).

Preparation of [(η^5-C_5Me_5)IrCl(L_2)]Cl (7). A mixture of [{(η^5-C_5Me_5)IrCl}$_2$(μ-Cl)$_2$] (200.0 mg, 0.251 mmol) and L_2 (130.7 mg, 0.502 mmol) in methanol (25 mL) was stirred for 2 h. The resulting solution was partially concentrated under reduced pressure. Slow addition of diethyl ether gave an orange microcrystalline solid, which was filtered off, washed with diethyl ether, and air-dried. Yield: 85% (**7a**:**7a′** molar ratio, 70:30). Anal. Calcd for $C_{28}H_{31}N_2Cl_2Ir\cdot 2H_2O$: C, 48.41; H, 5.08; N, 4.03. Found: C, 48.33; H, 5.00; N, 3.79. IR (Nujol, cm^{-1}): ν(CN) 1595 (s), ν(IrCl) 290 (s). **7a**: ^{1}H NMR ($(CD_3)_2CO$, for proton labeling, see Scheme 1) δ 1.71 (s, 15H, C_5Me_5), 2.18 (d, J_{H_aH} = 6.9 Hz, 3H, Me), 6.41 (q, 1H, H_a), 9.73 (s, 1H, H_b), 9.29 (d, J_{H_eH} = 5.4 Hz, 1H, H_f), 7.4−9.0 (aromatic protons of **7a** and **7a′**). **7a′**: ^{1}H NMR ($(CD_3)_2CO$) δ 1.75 (s, 15H, C_5Me_5), 2.09 (d, J_{H_aH} = 6.9 Hz, 3H, Me), 6.61 (q, 1H, H_a), 10.56 (s, 1H, H_b), 9.11 (d, J_{H_eH} = 5.1 Hz, 1H, H_f).

Preparation of [(η^5-C_5Me_5)IrCl(L_2)][A] (8−10). To a solution of a 70:30 mixture of **7a**:**7a′** (100.0 mg, 0.152 mmol) in 25 mL of methanol, the appropriate salt $NaBF_4$, $NaPF_6$, or HR*SO_3 and KOH (0.152 mmol) was added. The mixture was stirred for 1 h (24 h for complex **10**), and during this time, the precipitation of an orange solid was observed for complexes **8** and **9**. The resulting mixture was vacuum-evaporated to dryness. The residue was extracted with dichloromethane (15 mL), and the solution was partially concentrated under reduced pressure. Slow addition of diethyl ether gave an

orange microcrystalline solid, which was filtered off, washed with diethyl ether, and air-dried. Complex **8**. Yield: 68% (**8a**:**8a′**, 62:38). By recrystallization from methanol−diethyl ether, a 70:30 **8a**:**8a′** mixture was obtained. Anal. Calcd for $C_{28}H_{31}N_2BClF_4Ir\cdot H_2O$: C, 46.19; H, 4.57; N, 3.85. Found: C, 46.06; H, 3.85; N, 3.87. IR (Nujol, cm^{-1}): ν(CN) 1600 (s). **8a**: ^{1}H NMR ($(CD_3)_2CO$, for proton labeling, see Scheme 1) δ 1.81 (s, 15H, C_5Me_5), 2.10 (d, $J_{H_aH} = 6.9$ Hz, 3H, Me), 6.42 (q, 1H, H_a), 9.18 (d, $J_{H_eH} = 5.7$ Hz, 1H, H_f), 9.04 (d, $J_{H_aH} = 1.5$ Hz, 1H, H_b), 7.4−8.5 (aromatic protons of **8a** and **8a′**). **8a′**: ^{1}H NMR ($(CD_3)_2CO$) δ 1.76 (s, 15H, C_5Me_5), 2.15 (d, $J_{H_aH} = 7.2$ Hz, 3H, Me), 6.66 (q, 1H, H_a), 9.71 (s, 1H, H_b), 9.11 (d, $J_{H_eH} = 5.7$ Hz, 1H, H_f). Complex **9**. Yield: 70% (**9a**:**9a′**, 66:34). By recrystallization from methanol−diethyl ether, a 80:20 **9a**:**9a′** mixture was obtained. Anal. Calcd for $C_{28}H_{31}N_2ClF_6IrP$: C, 43.78; H, 4.07; N, 3.65. Found: C, 43.76; H, 3.80; N, 3.46. IR (Nujol, cm^{-1}): ν(CN) 1600 (s). **9a**: ^{1}H NMR ($(CD_3)_2CO$, for proton labeling, see Scheme 1) δ 1.82 (s, 15H, C_5Me_5), 2.10 (d, $J_{H_aH} = 6.8$ Hz, 3H, Me), 6.42 (q, 1H, H_a), 9.03 (s, 1H, H_b), 9.18 (d, $J_{H_eH} = 5.6$ Hz, 1H, H_f), 7.4−8.5 (aromatic protons of **9a** and **9a′**). **9a′**: ^{1}H NMR ($(CD_3)_2CO$) δ 1.76 (s, 15H, C_5Me_5), 2.15 (d, $J_{H_aH} = 7.0$ Hz, 3H, Me), 6.67 (q, 1H, H_a), 9.71 (s, 1H, H_b), 9.19 (d, $J_{H_eH} = 5.6$ Hz, 1H, H_f). Complex **10**. Yield: 77% (**10a**:**10a′**, 90:10). Anal. Calcd for $C_{37}H_{46}N_2ClIrO_4S\cdot H_2O$: C, 50.93; H, 5.54; N, 3.21. Found: C, 50.90; H, 5.04; N, 3.24. IR (Nujol, cm^{-1}): ν(CN) 1595 (s). **10a**: ^{1}H NMR ($(CD_3)_2CO$, for proton labeling, see Scheme 1) δ 1.74 (s, 15H, C_5Me_5), 2.10 (d, $J_{H_aH} = 7.2$ Hz, 3H, Me), 6.42 (q, 1H, H_a), 9.37 (s, 1H, H_b), 9.23 (d, $J_{H_eH} = 5.7$ Hz, 1H, H_f), 7.4−8.8 (aromatic protons of **10a** and **10a′**). **10a′**: ^{1}H NMR ($(CD_3)_2CO$) δ 1.76 (s, 15H, C_5Me_5), 2.15 (d, $J_{H_aH} = 7.0$ Hz, 3H, Me), 6.62 (q, 1H, H_a), 10.04 (s, 1H, H_b), 9.10 (d, $J_{H_eH} = 5.7$ Hz,1H, H_f).

Preparation of [(η^5-C_5Me_5)Ir(L_6)(H_2O)][SbF_6]$_2$ (11). To a 50:50 diastereomeric mixture of the chloro compound **6** (15.0 mg, 0.018 mmol), 6.13 mg (0.018 mmol) of $AgSbF_6$ in 0.7 mL of $(CD_3)_2CO$ was added. The suspension was stirred for 30 min. The AgCl formed was separated by filtration. The filtrate contained complex **11** in a 85:15 **11a**:**11a′** molar diastereomeric ratio. A ROESY experiment correlated free and coordinated water for **11a** and H_f, H_d, and H_e of **11a** with their corresponding protons in **11a′**. Complex **11a** (for proton labeling, see Figure 7): ^{1}H NMR ($(CD_3)_2CO$) δ 1.81 (s, 15H, C_5Me_5), 5.28 (m, 1H, H_a), 9.58 (s, 1H, H_b), 8.66 (d, $J_{H_dH} = 7.7$ Hz, 1H, H_c), 8.50 (t, $J_{H_eH} = 7.7$ Hz, 1H, H_d), 8.14 (m, 1H, H_e), 9.37 (d, $J_{H_eH} = 4.9$ Hz, 1H, H_f), 1.90 (m, 1H, H_h), 2.70 (m, 1H, H_g), 1.09 (s, 3H, Me_k), 1.01 (s, 3H, Me_j), 1.23 (s, 3H, Me_i), 7.65 (bs, 2H, H_2O). Selected ^{1}H−^{1}H COSY data: H_a correlated with H_g and H_g correlated with H_h. Selected NOE data (irradiated nucleus(i); enhanced protons (%)). H_a: H_g (6.0), C_5Me_5 (13.75), Me_i (9.5), Me_k (3.5), Me_j (1.4). H_b: H_c (11.45), H_e (4.4), H_h (9.6). H_g: H_a (7.9), H_h (12.0), C_5Me_5 (6.0), Me_i (5.6). H_h: H_b (4.35), H_f (0.95), H_g (8.2), Me_j (2.7). C_5Me_5: H_b (0.6), H_f (0.5), H_a (0.4), H_g (1.4), Me_j (0.4). Me_k: H_b (0.7), H_f (0.4), H_2O (0.5), H_a (1.45). H_2O: H_f (1.1), C_5Me_5 (3.9), Me_k (4.0). When the C_5Me_5 or H_h protons were irradiated, some CH_2 bornyl protons were also partially irradiated. Similarly, when the C_5Me_5 protons were irradiated, the H_h proton was also partially irradiated. Complex **11a′**: ^{1}H NMR ($(CD_3)_2CO$) δ 1.80 (s, 15H, C_5Me_5), 5.10 (m, 1H, H_a), 8.33 (m, 1H, H_d), 7.97 (m, 1H, H_e), 9.03 (m, 1H, H_f), 0.99 (s, 3H, Me), 1.18 (s, 3H, Me), 1.23 (s, 3H, Me).

Rate of Epimerization of 5a. The following procedure is representative. Complex **5a** (4.6 mg, 0.006 mmol) was dissolved in 0.7 mL of CD_3OD in a 5 mm NMR tube. The probe was heated to 45 °C, and rate data were acquired (48 spectra/12 h). The concentrations of **5a** and **5a′** were assayed by integration of the H_b resonances (δ 9.16 (**5a**), 8.99 (**5a′**)). Concentration ($\ln[C_o]-[C_\infty]/[C]-[C_\infty]$) vs time data were fitted by conventional linear regression methods ($k = (2.70 \pm 0.04) \times 10^{-5}$ s^{-1}). k values at different temperatures: k (49 °C) = $(3.48 \pm 0.08) \times 10^{-5}$ s^{-1}, k (55 °C) = $(7.89 \pm 0.07) \times 10^{-5}$ s^{-1}, k (59 °C) = $(1.20 \pm 0.02) \times 10^{-4}$ s^{-1}, k(62 °C) = $(1.70 \pm 0.02) \times 10^{-4}$ s^{-1}. The activation parameters ($\Delta H^{\ddagger} = 97.7 \pm 13.2$ kJ mol^{-1} and $\Delta S^{\ddagger} = -26.3 \pm 6.2$ J K^{-1} mol^{-1}) were obtained by a least-squares fit of the Eyring plot. The assumed errors were 2.6% in the rate constant and 1 K in the temperature. Errors were computed by published methods.[24]

Rate of Epimerization of 5a in the Presence of L_5. The following procedure is representative. Complex **5a** (4.6 mg, 0.006 mmol) and L_5 (8.0 mg, 0.037 mmol) were dissolved in 0.7 mL of CD_3OD in a 5 mm NMR tube. The probe was heated to 60 °C, and rate data were acquired (18 spectra/3 h). The concentrations of **5a** and **5a′** were assayed by integration of the H_b resonances. Concentration ($\ln[C_o]-[C_\infty]/[C]-[C_\infty]$) vs time data were fitted by conventional linear regression methods ($k = (1.55 \pm 0.01) \times 10^{-4}$ s^{-1}). Additional data for different amounts of L_5: 12.0 mg (0.055 mmol) of L_5, $k = (9.03 \pm 0.02) \times 10^{-5}$ s^{-1}; 16.0 mg (0.074 mmol) of L_5, $k = (1.11 \pm 0.01) \times 10^{-4}$ s^{-1}; 20.0 mg (0.092 mmol) of L_5, $k = (9.49 \pm 0.02) \times 10^{-5}$ s^{-1}; without L_5, $k = (1.28 \pm 0.05) \times 10^{-4}$ s^{-1}.

Rate of Epimerization of 5a in the Presence of NEt_4Cl. The following procedure is representative. Complex **5a** (4.6 mg, 0.006 mmol) and NEt_4Cl (6.0 mg, 0.036 mmol) were dissolved in 0.7 mL of CD_3OD in a 5 mm NMR tube. The probe was heated to 62 °C, and rate data were acquired (18 spectra/3 h). The concentrations of **5a** and **5a′** were assayed by integration of the H_b resonances. Concentration ($\ln[C_o]-[C_\infty]/[C]-[C_\infty]$) vs time data were fitted by conventional linear regression methods ($k = (1.96 \pm 0.02) \times 10^{-4}$ s^{-1}). Additional data for different amounts of NEt_4Cl: 9.0 mg (0.054 mmol) of NEt_4Cl, $k = (2.10 \pm 0.03) \times 10^{-4}$ s^{-1}; 12.0 mg (0.072 mmol) of NEt_4Cl, $k = (2.28 \pm 0.06) \times 10^{-4}$ s^{-1}; 15.0 mg (0.091 mmol) of NEt_4Cl, $k = (2.54 \pm 0.06) \times 10^{-4}$ s^{-1}; without NEt_4Cl, $k = (1.70 \pm 0.02) \times 10^{-4}$ s^{-1}.

Catalytic Diels−Alder Reaction between Methacrolein and Cyclopentadiene. The corresponding precatalyst **1**−**6**, **8**−**10** (0.025 mmol) in acetone/dichloromethane (0.2/2 mL) was treated with the appropriate silver salt (0.025 mmol), the resulting suspension stirred for 15 min, and the AgCl formed separated by filtration through Celite. The filtrate was kept under argon at the appropriate temperature. The dienophile (0.5 mmol in 2 mL of CH_2Cl_2) and freshly distilled cyclopentadiene (3 mmol in 2 mL of CH_2Cl_2) were added consecutively by syringe. The resulting solution was stirred at the reaction temperature and monitored by gas chromatography (GC). Yield and exo:endo ratio were determined by GC. The reaction mixture was concentrated to ca. 0.3 mL and filtered through silica gel washing with CH_2Cl_2/*n*-hexane (1/3) before the determination of the enantiomeric purity. Enantiomeric excesses (ee) were determined by integration of the aldehyde proton of both enantiomers using $Eu(hfc)_3$ as a chemical shift reagent ($Eu(hfc)_3$/adduct ratio, 0.3). The absolute configuration of the major adduct was assigned by comparing the sign of $[\alpha]_D$ with that of the literature.[25]

Crystal Structure Determination of Complexes 1a, 2a·$CHCl_3$, and 3a. A summary of crystal data, intensity collection and refinement parameters for the three structural analyses is reported in Table 5. An orange (**1a** and **2a**) or a dark-red crystal (**3a**) was glued to a glass fiber and mounted on a Siemens P4 diffractometer with graphite-monochromated Mo Kα radiation (λ = 0.710 73 Å). Cell constants were obtained from the least-squares fit on the setting angles of 44 reflections (25° ≤ 2θ ≤ 40°) for **1a**, 60 (20° ≤ 2θ ≤ 30°) for **2a** and 40 (25° ≤ 2θ ≤ 40°) for **3a**. A set of independent reflections with 2θ up to 59° (**1a**), 45° (**2a**), or 58° (**3a**) was measured using the ω/2θ scan technique (ω for **2a**) and corrected for Lorentz and polarization effects. Reflections were also corrected for absorption by a semiempirical method (Ψ-scan).[26] Three

(24) Morse, P. M.; Spencer, M. O.; Wilson, S. R.; Girolami, G. S. *Organometallics* **1994**, *13*, 1646.
(25) Furuta, K.; Shimizu, S.; Miwa, Y.; Yamamoto, H. *J. Org. Chem.* **1989**, *54*, 1481.

Table 5. Crystal Data and Data Collection and Refinement for 1a, 2a, and 3a

	1a	2a	3a
chem formula	$C_{24}H_{29}ClF_6IrN_2Sb$	$C_{28}H_{31}ClF_6IrN_2Sb\cdot CHCl_3$	$C_{32}H_{33}ClF_6IrN_2Sb$
fw	808.89	978.32	909.00
cryst size, mm	0.48 × 0.44 × 0.20	0.25 × 0.20 × 0.15	0.38 × 0.34 × 0.28
cryst syst	monoclinic	orthorhombic	orthorhombic
space group	$P2_1$	$P2_12_12_1$	$P2_12_12_1$
a, Å	8.380(2)	10.7605(12)	11.835(2)
b, Å	10.358(2)	13.3931(13)	12.445(2)
c, Å	15.841(3)	23.627(3)	21.323(4)
β, deg	99.85(3)	90	90
V, Å^3	1354.7(5)	3405.0(6)	3140.6(9)
Z	2	4	4
D_{calcd}, g cm^{-3}	1.983	1.908	1.922
μ, mm^{-1}	6.059	5.067	5.239
scan type	$\omega/2\theta$	ω	$\omega/2\theta$
θ range, deg	2.4−29.5	2.1−22.5	1.9−29.0
temp, K	200.0(2)	150.0(2)	200.0(2)
no. of measd reflns	8373	5134	9251
no. of unique reflns	7539 (R_{int} = 0.0162)	4402 (R_{int} = 0.0564)	8283 (R_{int} = 0.0154)
min, max trasm factors[a]	0.047, 0.105	0.189, 0.217	0.055, 0.085
no. data/restraints/params	7539/56/368	4402/77/396	8283/36/400
$R(F)$ ($F^2 \geq 2\sigma(F^2)$)[b]	0.0280	0.0469	0.0296
w$R(F^2)$ (all data)[c]	0.0688	0.1067	0.0640
S[d]	1.002	0.912	0.945

[a] A semiempirical ψ-scan absorption correction was applied. [b] $R(F) = \sum||F_o| - |F_c||/\sum|F_o|$ for 7119 (**1a**), 3133 (**2a**), and 7326 (**3a**) observed reflections. [c] $wR(F^2) = [\sum[w(F_o^2 - F_c^2)^2]/\sum[w(F_o^2)^2]]^{1/2}$; $w^{-1} = [\sigma^2(F_o^2) + (aP)^2]$, where $P = [\max(F_o^2, 0) + 2F_c^2)]/3$ (**1a**, a = 0.0527; **2a**, a 0.0557; **3a**, a = 0.0356). [d] $S = [\sum[w(F_o^2 - F_c^2)^2]/(n - p)]^{1/2}$, where n is the number of reflections and p the number of parameters.

standard reflections were monitored every 100 measurements throughout data collection as a check on crystal and instrument stability; no significant variation was observed.

All of the structures were solved by direct methods and subsequent difference Fourier techniques (SHELXTL-PLUS)[27] and refined by full-matrix least-squares on F^2 (SHELXL-97).[28] In the three crystal structures the SbF_6^- counteranions were observed heavily disordered. They were modeled with two (**2a** and **3a**) or three (**1a**) different SF_6 moieties, which were refined with feeble geometrical restraints (DFIX applied to Sb−F and F···F distances) and complementary occupancy factors. A chloroform solvent molecule was found in the crystal structure of **2a**; this molecule was also observed disordered and included in the refinement distributed in two positions with complementary occupancy factors. Anisotropic thermal parameters were used in the last cycles of refinement for all non-hydrogen atoms, except for the fluoride atoms of the anionic SbF_6^- groups involved in disorder and the $CHCl_3$ atoms in **2a**. Hydrogen atoms of the terminal methyl groups were placed at their calculated positions; the remaining ones were obtained from difference Fourier maps. All were refined riding on carbon atoms with one (**2a**) or four (**1a** and **3a**) common isotropic displacement parameters. The function minimized was $\sum[w(F_o^2 - F_c^2)^2]$. The calculated weighting scheme was $1/[\sigma^2(F_o^2) + (aP)^2]$, where $P = [\max(F_o^2,0) + 2F_c^2)]/3$. All of the refinements converged to reasonable R factors (Table 5). In the three crystals the absolute structure has been checked by the estimation of the Flack parameter x in the final cycles of refinement, 0.009(5) (**1a**), −0.017(15) (**2a**), and −0.011(5) (**3a**).[29] The highest remaining peaks in the final difference maps of 1.44 (**1a**), 0.97 (**2a**), and 0.87 (**3a**) e/Å^3 were situated in close proximity to the metal centers and have no chemical sense. Scattering factors were used as implemented in the refinement program.[28]

Acknowledgment. We thank the Dirección General de Investigación Científica y Técnica for financial support (Grant No. PB96/0845).

Supporting Information Available: Full tables of crystallographic data, complete atomic coordinates, isotropic and anisotropic thermal parameters, and bond distances and angles for complexes **1a**, **2a**, and **3a** (33 pages). X-ray crystallographic files, in CIF format, for **1a**, **2a**, and **3a**, are available through the Internet only. Ordering and Internet access information is given on any current masthead page.

OM980112N

(26) North, A. C. T.; Phillips, D. C.; Mathews, F. S. *Acta Crystallogr., Sect. A* **1968**, *24*, 351.
(27) Sheldrick, G. M. *SHELXTL-PLUS*; Siemens Analytical X-ray Instruments: Madison, WI, 1990.
(28) Sheldrick, G. M. *SHELXL-97, Program for Crystal Structure Refinement*; University of Göttingen: Göttingen, Germany, **1997**.
(29) Flack, H. D. *Acta Crystallogr.* **1983**, *A39*, 876.